



1 Meteorological factors driven glacial till changing and the associated
2 periglacial debris flows in Tianmo Valley, southeast Tibetan Plateau

3 Mingfeng Deng^{1,2}, Ningsheng Chen^{1*}, and Mei Liu^{1,2}

4 ¹ Key Laboratory of Mountain Hazards and Surface Process, Institute of Mountain Hazards and Environment,
5 Chinese Academy of Sciences, Chengdu 610041, China;
6 ² University of Chinese Academic of Sciences, Beijing 100049, China)

7 Abstract: Meteorological studies have indicated that high Alpines are strongly affected by climate
8 warming. Periglacial debris flows are more frequent in deglaciated regions. The combination of
9 rainfall and air temperature controls the initiation of periglacial debris flows; and the addition of
10 melt-water due to higher air temperatures enhances the complexity of the triggering mechanism
11 compared to storm-induced debris flows. In south-eastern Tibetan Plateau where temperate
12 glaciers are widely distributed, numerous periglacial debris flows have occurred in the past 100
13 years, but none had happened in the Tianmo watershed until 2007. In 2007 and 2010, three
14 large-scale debris flows occurred in the Tianmo watershed. In this research, these three debris flow
15 events were chosen to analyze the impact of the annual meteorological conditions: the antecedent
16 air temperature and meteorological triggers. TM images and field measurement of the nearby
17 glacier suggested that a sharp glacier retreat had existed in the previous one or two years
18 preceding the events, which coincided with the spiked annual air temperature. Besides, changing
19 of glacial tills driven by prolonged increase in the air temperature is the prerequisite of periglacial
20 debris flows. Triggers of periglacial debris flows are multiplied and they could be high intensity
21 rainfall as in DF1 and DF3, or continuous percolation of melt-water due to the long term rising air
22 temperatures as in DF2.

23 **1. Introduction**

24 The alpine environments are strongly vulnerable to climate changes, of which the
25 alpine glaciers and permafrost are the most sensitive in the form of glacier and
26 permafrost retreat (Harris et al, 2009; IPCC, 2013). Glacier and permafrost retreat can
27 induce mass movement, such as landslides, shallow slides, debris, moraine collapses,
28 etc. (Cruden and Hu, 1993; Korup, 2009; McColl, 2012; Stoffel and Huggel, 2012;
29 Fischer et al, 2012), that will be expelled out of the watershed in the form of debris
30 flows or sediment flux. The debris flow in alpine areas can often bury residential areas,
31 cut off main roads and block rivers (Shang et al, 2003; Cheng et al, 2005; Deng et al,



32 2013) and destroy basic facilities located in downstream, posing a great threat to the
33 local economy and social development. In undeveloped alpine areas such as the
34 south-eastern Tibet where the traffic/drainage system is particularly poor or limited,
35 the negative effects produced by debris flows such as cutting off main roads are
36 serious (Cheng et al, 2005).

37 Periglacial debris flows characterize the high alpine areas containing large areas
38 of glaciers, such as the Tibetan Plateau in China(Shang et al, 2003; Ge et al, 2014),
39 Alps in Europe(Sattler et al, 2011; Stoffel and Huggel,2012), Caucasus Mountains in
40 Russia(Evans et al, 2009) and northern Canada(Lewkowicz1 and Harris, 2005).
41 Periglacial debris flows were reported to be initiated by rainfall (Stoffel et al, 2011;
42 Schneuwly-Bollschweiler and Stoffel, 2012), melt-water flow of glacier or ice particle
43 ablation(Arenson and Springman, 2005; Decaulne et al, 2005), or outburst floods
44 from glacier lakes (Chiarle et al, 2007) in different parts of the world, while the
45 multi-triggers for the case is rarely to be read. Because debris flows are commonly
46 triggered by rainfall (Sassa and Wang, 2005; Decaulne et al, 2007; Kean et al, 2013;
47 Takahashi, 2014), the rainfall threshold, intensity and duration has been widely used
48 for debris flow monitoring and giving warning in non-glacier areas (Guzzetti et al,
49 2008).

50 In deglaciation areas, the debris flow threshold can be more difficult to determine.
51 Periglacial debris flows tend to occur in the summer when the thawing of glaciers and
52 glacial tills predominates and melt-water penetrates into the glacial tills at a constant
53 and successive flow. The effect of melt-water appears similar to that of antecedent
54 rainfall (Rahardjo et al, 2008) and is variable in different periods, considering snow
55 and glacier shrinkage and air temperature fluctuation. In the Swiss Alps, melt-water is
56 high in early summer, and as debris flows can be initiated by low total rainstorm,
57 whereas higher total rainstorm are required in late summer or early autumn when the
58 melt-water is low (Stoffel et al, 2011; Schneuwly-Bollschweiler and Stoffel, 2012). In
59 south-eastern Tibetan Plateau, the rainfall threshold given by Chen et al., (2011) is
60 quite wide, and the small rainfall threshold in particular is likely to contain the effect
61 of air temperature. Moreover, periglacial debris flows induced by a sudden release of



62 water from dammed glaciers have a close relationship with the rising air temperature
63 (Liu et al, 2014).

64 Fluctuation of air temperature is likely to be quite important in triggering
65 periglacial debris flows. Compared with the storm induced debris flows, the addition
66 of air temperature can greatly enhance the complexity of the initiation of periglacial
67 debris flows. It is of high difficulty to simulate the triggering process by experiment
68 or mathematical simulation, and instead, debris flows cases in the natural environment
69 could be the perfect object. In this research, three debris flow events, after a
70 debris-flow-free period of nearly 100-year, in the Tianmo watershed of the
71 southeastern of the Tibetan Plateau as deglaciation continued are used as examples,
72 and the annual meteorological conditions, antecedent air temperature and triggering
73 conditions prior to debris flows are analyzed to further understand the meteorological
74 triggers and their roles in glacier retreat, glacial till change and debris flow initiation.

75 **2. Background**

76 **(1) Study area**

77 The temperate glacier in the Tibetan Plateau is primarily distributed in the
78 Parlung Zangbo Basin and covered a total landmass of 2381.47 km² in 2010 based on
79 TM images (Liu, 2013). Historically, the movement of temperate glacier has produced
80 a large amount of moraines, the depth of which can reach up to 500 m locally (Yuan et
81 al, 2007). In recent decades, there has been a dynamic significant increase in
82 temperature and according to statistics the temperature at the Bomi meteorological
83 station (midstream in the Parlung Zangbo Basin) has rose by 0.23°C/10a from 1969 to
84 2007, resulting in remarkable shrinkage of the glacier(Yang et al, 2010).

85 Tianmo Valley, located in Bomi County and to the south of the Parlung Zangbo
86 River, covers an area of 17.76 km² (29°59'N/95°19'E; Figure 1). This valley has a
87 northeast-southeast orientation and is surrounded by high mountains reaching 5590 m
88 a.s.l. at the southernmost site and 2460 m a.s.l. at the junction of the Parlung Zangbo
89 River. The TM image in 2013 showed the presence of a hanging glacier with an area



90 of 1.42 km² in the upper concave area at an altitude of 4246 m to 4934 m. Bared rock,
91 dipping at an angle of around 60°, emerged below and above the hanging glacier and
92 often covered by everlasting snow. Below 3800m a.s.l., vegetation, including forest
93 and shrub, occupies most of the area (Table 1).

94 The river channel in the watershed is sheltered by shade and not directly affected
95 by sunlight, resulting in less solar radiation and a location at which a small trough
96 glacier can form. In the main channel, the trough glacier extended to 2966 m a.s.l. in
97 2006. The lower part of the trough glacier has been eroded by glacier melt-water flow,
98 and an arch glacier that is vulnerable to high pressure was formed (Figure 2). The
99 remnants of the landslide deposits approximately 10 meters high, which consist of low
100 stability sediment and can be easily entrained by debris flows, can be observed in both
101 sides of the channel.

102 Tianmo Valley is on the north side of the bend in the Yarlung Zangbo River and
103 is strongly affected by the new tectonic movement. An inferred normal fault vertical
104 to the channel cuts through the valley and is only 30 km away from the Yarlung
105 Zangbo fault. In 1950, a rather significant earthquake (Ms. 8.6) hit Zayu, which is
106 only 200 km away, and local records reported that a large amount of rock collapsed
107 and landslides were produced at that time. The whole valley is in a strong ductile
108 deformation zone and is dominated by gneissic lithology belonging to Presinian
109 System.

110 (2) Disaster history

111 According to our field interview with local residents, there were no debris flows
112 in approximately 100 years prior to 2007 in Tianmo Valley. The channel was quite
113 narrow before 2007, and the local people could walk across via a wooden bridge to
114 live and farm on the terrace on the west side. The ecology was in a rather peaceful
115 state at that time.

116 On the morning of Sep. 4th, 2007, after the rainfall which did not hit the
117 downstream area ceased, the local forest guard heard a loud noise coming from the
118 upstream area at approximately 18:00; with rainfall which later began in the upstream



119 area at approximately 19:00, following this rainfall was debris flows which rushed out
120 of the Tianmo Channel and subsequently blocked the Parlung Zangbo River; report
121 stated that several debris flows occurred, lasting the entire night. According to the
122 field measurements, approximately 1,340,000 m³ of sediment was transported during
123 this event, resulting in 8 missing persons and deaths. Concurrently within this same
124 time, debris flows occurred in the four nearby valleys (Table 2). According to the size
125 classification proposed by Jakob (2005), which is based on the total volume, peak
126 discharge and inundated area, Size class of debris flows in the five valleys is given in
127 Table 2.

128 At 11:30 on Jul. 25th, 2010, debris flows were again triggered in Tianmo Valley
129 that traced the path of the preceding debris flow deposits and reached the other side of
130 the Parlung Zangbo River. According to Ge et al., (2014), solid mass sediment of
131 approximately 500,000 m³ was carried out (Table 1) and deposited on the cone to
132 block the main river. A barrier lake was formed, and the rising water destroyed the
133 roadbed of G318. The following week also experienced dozens of debris flows in
134 small magnitude.

135 Debris flows occurred again two months later on Sep. 6th (The Ministry of Land
136 and Resources P. R. C., 2010), although we could not determine the exact times
137 sequence of event but according to speculation, these debris flows could have
138 occurred in the early morning before dawn and when the rainfall intensity has reached
139 its maximum(Figure 9), which agrees with the findings of Chen (1991) that periglacial
140 debris flows have historically occurred between 18:00~24:00 in this area. The debris
141 barrier in the main river was consequently increased by an additional 450,000 m³, and
142 the barrier lake was enlarged to maintain 9,000,000 m³ of water.

143 A field investigation revealed that a high percentage of boulders in the
144 downstream area and glacial tills above the trough glacier were quite loose and of
145 high porosity (Figure 2), hence they have low density and can be easily entrained. Our
146 particle size tests on the glacial tills and debris flow deposits indicate a lower clay
147 (d<0.005 mm) content, whereas the debris flow deposits contain more fine particles
148 that are smaller than 10 mm (Figure 4), suggesting that the entrainment supplied a



149 considerable amount of fine particles.

150 **(3) Meteorological data**

151 The study area is located in a high alpine area where the economy is quite
152 undeveloped with only few meteorological stations. Before 2011, the Bomi
153 meteorological station was the only station in the area, located 54 km away from
154 Tianmo valley at an altitude of 2730 m, and other stations were located more than 200
155 km away.

156 The Tibetan Plateau is a massive terrace that obstructs the Indian monsoon,
157 causing it to travel through the Yarlung Zangbo Canyon and its tributaries. As the
158 Indian monsoon is transported to higher altitudes, a rainfall gradient emerges in the
159 Parlung Zangbo Basin. However, according to our statistics on rainfall data in the area,
160 the rainfall is more or less the same from Guxiang to Songzong considering the
161 long-term rainfall process; therefore, the rainfall data from the Bomi meteorological
162 station can be used for our study. In order to conduct further study, another
163 meteorological station was built in 2011 near Tianmo Valley.

164 It has been established that the air temperature decreases with altitude; therefore
165 the air temperature in the source area of Tianmo Valley is lower than that in Bomi
166 County. According to the research by Li and Xie (2006), the air temperature decreases
167 at a rate of (0.46~0.69)°C/100m over the whole Tibetan Plateau, and the rate in the
168 study area is 0.54°C/100 m. Because the glacier and permafrost in the source area
169 have a planar distribution, the air temperature at the geometric centre of the glacier
170 and permafrost can be used to analyze the temperature process.

171 **3. Analysis and results**

172 **(1) Changing of air temperature and rainfall**

173 The annual air temperature is usually used to reflect the tendency of glacier
174 change (Yang et al, 2015). We collected annual air temperature and annual rainfall
175 data from 1970 to 2014 from the Bomi meteorological station (Figure 5). The record



176 showed that the overall air temperature has increased by approximately 1.5°C in the
177 last 45 years, accounting for 0.033°C/a. This air temperature increase was particularly
178 more rapid between 2005~2007, an approximately 0.7°C/3a, which is 7 times the
179 average value of the last 45 years. On the other hand, the annual rainfall from 2000 to
180 2010 was low and it was estimated at 828.2 mm per year. From 2000 to 2004, the
181 rainfall during summer (July to September) accounted for approximately 50% of the
182 total annual rainfall; however, only 32% of the rainfall occurred in the summer of
183 2005~2006, even though the annual rainfall exhibited the same trend. In 2007, the
184 rainfall in the summer and the entire year returned to normal.

185 According to Figure 5, a similar trend in the air temperature and rainfall was
186 observed before DF2 and DF3. The air temperature elevated in 2009 to reach the
187 maximum of the last 45 year period, accounting for 10.2 °C; however, the annual
188 rainfall, was only 65% of the average amount; and the summer rainfall, lower than
189 that in 2005 and 2006, reached their minimum values. In 2010, the rainfall was
190 abundant and the annual rainfall increased to 1080.6 mm, which is approximately 30%
191 more than the average value and close to the maximum.

192 The following common traits can be identified from comparing the annual
193 meteorological conditions of DF1, DF2 and DF3. 1) One or two years before the
194 debris flows, the annual temperature elevated and the annual rainfall and summer
195 rainfall increased. The climate was in a "hot-dry" state. 2) As the temperature
196 gradually decreased, the annual rainfall returned to normal or increased, and the
197 "hot-wet" climate contributed to debris flow initiation (Lu and Li, 1989).

198 **(2) Changing of glacier in Tianmo valley**

199 In our research, remote image is collected to analyze the changing of glacier in
200 the source area during the past years. In order to eliminate the effect of snow cover,
201 images were taken in the thawing seasons when the snow cover is limited to enable an
202 easy detection of the glacier from snow. Besides, a bright cloud is still needed to show
203 the watershed clearly; however a difficult case ensues when the rainy season comes
204 in-between the thawing season when the atmosphere is often covered by thick cloud.



205 Further, in order to show glacier retreat and its impact on debris flows properly, the
206 images should be within similar time interval, like 3 years, before and after debris
207 flow events. As the high resolution images are rare to obtain and we could only collect
208 one SPOT in 2008. To achieve consistency of the images, we collected 5 TM images,
209 taken on Sep. 17th, 2000, Jul. 24th, 2003, Sep. 21st, 2006, Sep. 24th, 2009 and Aug. 4th,
210 2013, respectively.

211 Based on the 5 TM images, we classified the area as glacier, snow, bared land,
212 gully deposition and vegetation in time series (Figure 6), and the area of each is given
213 in Table 1. Figure 6 showed that deglaciation was taking place in Tianmo valley and
214 in particular, the eastern branch had experienced the sharpest deglaciation. In order to
215 show clearly the rapid rate of glacier retreat, a graph was plotted to show the changing
216 of glacier and the eastern branch in Figure 7.

217 Figure 7 shows that glacier in Tianmo valley had been in shrinkage since 2000 to
218 2013, with variation in glacier retreat rate. In 2000~2003, 2003~2006, 2006~2009 and
219 2009~2013, the glacier retreat rate in Tianmo valley corresponds to 0.02, 0.06, 0.027
220 and 0.0075km²/a and 0.0033, 0.01, 0.008 and 0.002 km²/a for the eastern branch.
221 According to these figures the largest glacier retreat rate was in 2003~2006, followed
222 by that in 2006~2009. It is important that glacier area at the beginning should be taken
223 into consideration to judge the changing rate of glacier. The glacier retreat rate is
224 normalized and the relative glacier retreat rate is defined as:

$$225 \quad D = \frac{(A_0 - A_1)}{nA_0} \quad (1)$$

226 Where D is the relative glacier retreat rate, km²/a/km²; A_0 is glacier area at the beginning,
227 km²; A_1 is glacier area at the end, km²; n is the duration of year, a.

228 The relative glacier retreat rate are 11.30, 35.09, 17.43 and 5.17 10⁻³km²/a/km²
229 during 2000~2003, 2003~2006, 2006~2009 and 2009~2013, respectively; whereas, it
230 is 20.83, 66.67, 66.67 and 20.83 10⁻³km²/a/km² for the eastern branch. These figures
231 show that the relative glacier retreat rate for the eastern branch had shrunk much more
232 sharply between 2000 ~2013.



233 In this research, TM images with 3 year intervals were applied can only get the
234 mean glacier retreat rate. As glacier retreat rate in the 3 three years could be either
235 high or low, field measurement of the nearby glacier is used to show the glacier retreat
236 condition before debris flows. Yang et al.(2015) had conducted field measurement of
237 No.94 Glacier in Parlung Zangbo Basin since 2006 and the field measurement
238 suggests it was in negative balance in 2006~2010(Figure 7). The negative balance
239 reached the maximal in 2009, followed by 2008 and 2006, indicating sharp
240 deglaciation in these three years.

241 When we combined the result of TM image and filed measurement of No. 94
242 Glacier, we observed that it is right before debris flows that glacier in Tianmo valley
243 experienced the sharpest deglaciation in 2006, 2008 and 2009, which was also
244 coincidental with the elevated annual air temperature (Figure 5). Besides, the
245 maximum glacier retreat in 2009 could be also related to the decline of snowfall in the
246 preceding winter and early spring and its increase may also have aided the glacier
247 retreat in 2007 and 2010.

248 **(3) Antecedent air temperature and rainfall process**

249 The air temperature in the source area can be obtained using the vertical decline
250 rate (0.54°C/100 m). According to this method, the air temperature in the source area
251 was 9.8°C lower than that at the Bomi meteorological station. We collected the daily
252 temperature; that is the lowest temperature, the mean temperature and daily rainfall
253 from June to September in 2007 and 2010 (Figure 8).

254 According to Figure 8, the lowest air temperature was below 0 at the end of June,
255 2007. At the beginning of July, the air temperature started to rise quickly which
256 continued until early September when DF1 occurred, this demonstrates that the high
257 air temperature in July and August contributed to DF1.

258 According to Figure 8, the air temperature was high from early July to late
259 August, and another high air temperature period emerged in early September. When
260 DF2 occurred in late July the air temperature had reached the maximum for that year,
261 which suggests that the air temperature in early and middle July was responsible for



262 DF2. After DF2 occurred, the air temperature in August began to prepare for DF3.
263 Antecedent air temperature fluctuation includes the air temperature and its
264 duration. The air temperature and duration before debris flows are variable, making
265 them difficult to evaluate. The accumulation of positive air temperature is usually
266 applied to analyze the impact of air temperature on glacier melting (Rango and
267 Martinec, 1995), which can be expressed as:

$$268 T_{PT} = \sum_{i=-n}^0 T_i (T_i > 0) \quad (2)$$

269 Where T_{PT} is the positive air temperature accumulation, °C and T_i is the
270 average daily air temperature; only $T_i > 0$ is included.

271 Because air temperature is successive, it is difficult to determine the beginning of
272 positive air temperature accumulation. Glacial tills can lessen the heat that penetrates
273 into them, and the low air temperature can only contribute to the upper thin layer;
274 moreover, freeze-thaw cycles exist when the lowest air temperature is less than 0°C.
275 From this point of view, the beginning of positive air temperature accumulation is
276 defined as the time at which the lowest air temperature exceeds 0°C for several
277 successive days or the last debris flow.

278 Based on the above method, we can deduce that the positive air temperature
279 accumulation began when the lowest air temperature exceeded 0°C for several
280 successive days, starting on June 28th, 2007 and June 9th, 2010 corresponding to DF1
281 and DF2, respectively, and on July 26th, 2010 for DF3, following DF2. The duration
282 and T_{PT} were calculated for each debris flow event, the result was 69 days and
283 517.9°C, 47 days and 332.1°C, 42 days and 320.4°C (Figure 8) for DF1, DF2, and
284 DF3, respectively. The result showed that T_{PT} for DF1 is much larger than the other
285 two, and the reasons for this may lie in the watershed there had been no debris flows
286 in the past dozens of years and only extraordinary external forces could have
287 destroyed the long-term balance.



288 (4) Triggering conditions

289 The continuous nature of the air temperature limits the possibility for debris
290 flows triggered by a sole abrupt increase in air temperature; and since the previous air
291 temperature trend cannot be neglected, it is of no sense to study air temperature
292 triggers.

293 Antecedent rainfall is a factor that favours debris flows. In our analysis, the
294 rainfall over the three days preceding a debris flow event is given in Figure 9.

295 Before DF1, the air temperature was high, and continued through July and
296 August. The T_{PT} reached 517.9°C. According to the local forest guard, an isolated
297 convective storm occurred prior to DF1 though no rainfall was recorded at the Bomi
298 meteorological station or in the downstream area at that time. In Figure 9, as the
299 rainfall right before DF1 occurred was not recorded by Bomi metrological station, we
300 added to the rainfall intensity (like 5 mm/h) before DF1 to account for the storm,
301 which does not reflect the rainfall during storm conditions. We can therefore conclude
302 that this isolated convective storm initiated DF1, while the long-term high air
303 temperature trend had paved the road for DF1. Considering a large deglaciated area,
304 several other periglacial debris flows simultaneously also occurred near Tianmo
305 Valley (Deng et al, 2013), which suggests the advantageous meteorological conditions
306 for debris flow initiation.

307 DF2 took place when the air temperature reached the peak in 2010. The thaw
308 season began in the middle of June, and the T_{PT} reached 332.1°C. On July 24th, one
309 day before DF2, the air temperature reached the maximum value for that year. The
310 rainfall record at the Bomi meteorological station shows that there had been no
311 rainfall several days preceding DF2, and the local citizens also did not observe any
312 rain either. The trigger of DF2 was likely the continuous percolation of melt-water
313 due to the long term rising air temperature.

314 According to field interviews, several debris flows of small magnitude had also
315 occurred before DF3. The air temperature decreased in late August but increased to



316 another high peak before DF3, and the T_{PT} reached 320.4°C. Rainfall began 2 days
317 prior to DF3 and was steady the entire day before DF3. According to the rainfall trend
318 at the Bomi meteorological station, the rapid increase in rainfall intensity started 4
319 hours before DF3 and reached 3.8 mm/h, which was responsible for the initiation of
320 DF3.

321 **4. Discussion**

322 Debris flows initiation is the process when water source provokes the movement
323 of soil mass. In this research, we found that the three debris flows were triggered by
324 high air temperature and rainfall in DF1, high air temperature in DF2, and rainfall in
325 DF3 respectively. When we analyzed the date and the triggers for these events,
326 various questions came to mind that gave reasons to doubts: 1) Why debris flows did
327 not occur in 2006 or 2009 when deglaciation reached its peak and more ice melt water
328 was present; 2) Why DF1 and DF3 occurred in September when the air temperature
329 and the ice melt water was decreasing; 3) Why was there is no large scale debris flows
330 triggered by the previous heavier storm. It makes us believe that the impact of water
331 source on the magnitude and frequency of debris flows is quite low, or there could be
332 much more debris flows; and instead, soil source, including its magnitude and activity,
333 should be the predominate controller, just as Jakob et al., (2005) pointed out that the
334 recharge of channel should be the prerequisite for debris flows. However, in most
335 situations we cannot reach the source area to detect the soil source and the high-tech
336 remote sensing can just distinguish the scope of soil source. In the preriglacial area
337 where the glacial till is often covered by glacier or everlasting snow, changing of soil
338 source seems to be of high difficulty to detect. In this research, we try to combine the
339 meteorological condition and the literatures to discuss the probable change of glacial
340 tills before debris flows.

341 **(1) Changing of glacial till in annual years**

342 Climate warming is a global trend (IPCC, 2013), and the Tibetan Plateau, as the
343 third pole, is no exception. According to our statistics, the air temperature in Bomi



344 County has increased by 1.5° in the last 45 years (1970~2014). Glacier retreat induced
345 by climate warming has been widely accepted, and recent research suggests the
346 weaker Indian monsoon could be another reason (Yao et al, 2012). Glaciers are
347 always located in concave ground and cover a large amount of glacial tills.
348 Gravitation of the glacier can generate normal stress vertical to the slope, which can
349 strengthen the slope stability. The effect of glaciers on slope stability is called glacial
350 debuttressing (Cossart et al, 2008). As deglaciation continues, the result could lead to
351 exposure of the frozen glacial tills (Figure 10, A to B) and smaller glacial
352 debuttressing.

353 The retreat of glaciers and glacial tills with climate warming is quite different.
354 Deglaciation is accompanied by melting of internal ice particles. The internal ice
355 particles are covered by active glacial till and though the effect of heat fluxes are
356 strong at the surface and quite limited in deep layers, resulting into the melting of
357 internal ice particles lagging behind glacial retreat (Hagg et al, 2008). Glacial till with
358 thicker coverage has a relatively thinner thawing layer, although the ablation rate of
359 glaciers and internal ice particles remain at the same pace at the junction with the
360 slope. Newly formed bared glacial till is of high ice content and frozen, the cohesion
361 of the ice particles renders the bared glacial till with high shearing strength and
362 stability. Therefore, we often see many bare moraine slopes near glaciers, for this
363 reason there were no debris flows of large magnitude in 2006 and 2009 when glacier
364 retreat reached the maximal.

365 **(2) Changing of glacial till in antecedent days**

366 After the long term cold winter, the whole glacial tills would become frozen. If
367 the regressive glacier was not recovered in the winter, the glacial tills would often be
368 covered by snow. As air temperature increases again, the surface snow would melt
369 first, followed by the internal ice particles. The thawing of internal ice particles would
370 induces a series of changes in the glacial till, which include the following: 1) the
371 thawing will break the bonds of ice particles and increase the instability between ice
372 cracks (Ryzhkin and Petrenko, 1997; Davies et al, 2001); 2) the sharp air temperature



373 fluctuation in high alpine mountainous areas induces a repeated cycle of expansion
374 and contraction in the glacial till that can destroy the mass structure to some extent; 3)
375 the seepage of ice melt-water can deliver fine-grained sediments that were formerly
376 frozen in the ice matrix (Rist, 2007); and 4) the ice melt-water can result in a higher
377 water content and pore water pressure (Christian et al, 2012). These changes in glacial
378 till can sharply decline the soil strength, shifting to an active mass from the uncovered
379 and frozen moraine (Figure 10, B to C). Because the heat conduction in glacial till is
380 quite slow, this process may last for a very long time and also requires a high
381 antecedent air temperature.

382 Heat conduction via the percolation of rainfall and ice melt-water can amplify
383 the scope of an active of glacial till (Gruber and Haeberli, 2007), whereas the shelter
384 of surface glacial till can hinder the heat flux from the internal mass. At a low air
385 temperature, the heat flux should be constrained to the surface layer, and a large heat
386 gradient due to a high air temperature would contribute much more to the heat flux
387 and ice melt in the deep mass, meaning that the long-term effect of a high air
388 temperature can amplify the active glacial till (Åkerman et al, 2008), under which lies
389 frozen glacial till with a high ice content. The activity of glacial till changes with
390 depth, high in the surface and low in the deep layers, and landslide failure can take
391 place on glacial till slopes in a stepwise manner, coinciding with long-term air
392 temperature fluctuations although the glacial till is significantly unlimited in
393 deglaciation areas.

394 (3) Failure of glacial tills

395 Active glacial till slopes with low strength are usually vulnerable, and their
396 failure can occur when the air temperature is above 0°C (Arenson and Springman,
397 2005). Either rainfall, the seepage flow of glacier or ice particle melt-water induced
398 by prolonged high air temperature could trigger the failure (Figure10, C to D). The
399 failure mechanism lies in the ablation of internal ice particles and the percolation of
400 melt-water that further decreases the soil strength at first (Arenson and Springman,
401 2005; Decaulne et al, 2005); later, the subsequent rapid percolation of melt-water or



402 rainfall can saturate the glacial till and initiate failure through the decrease of soil
403 suction and shearing strength (Springman et al, 2003; Decaulne and Sæmundsson,
404 2007; Chiarle et al, 2007).

405 The fluctuation of air temperature within a specific low range result into limited
406 seepage flow. Based on the hypothesis that the glacier is limited, it is unlikely for
407 failure to be triggered by short-term increases in air temperature; although prolong air
408 temperature increases can still trigger it. Rainfall can initiate debris flows from active
409 glacial tills with a mechanism similar to that of storm-induced debris flows in
410 non-glacier areas (Iverson et al, 1997; Springman et al, 2003; Sassa and Wang, 2005).
411 In the European Alps, periglacial debris flows are mainly provoked by rainfall, which
412 is also related with air temperature fluxes (Stoffel et al, 2011). The different portion
413 containing melt-water percolation would impact the rainfall intensity and duration
414 required for periglacial debris flows (Stoffel et al, 2011; Schneuwly-Bollschweiler and
415 Stoffel, 2012); Rainfall intensity and duration may also require other preconditions,
416 such as the distribution of glaciers and frozen glacial tills and the terrain of the source
417 area to enhance the debris flow (Lewkowicz and Harris, 2005).

418 The three debris flow events possess similar annual meteorological conditions,
419 except that the positive air temperature accumulation prior to DF1 was significantly
420 larger. DF1 occurred at the end of a prolonged period of high air temperature, prior to
421 this, there were instances of failure but no large-scale debris flows. On July 25th 2010
422 when the daily rainfall particularly reached 20.7 mm, no debris flows were generated
423 because thick active glacial till was still lacking after small failure events. In 2010, the
424 largest daily rainfall occurred on June 7th, accounting for 37.5 mm, at the beginning of
425 an air temperature increase when the glacial till was frozen and had low activity. The
426 lack of glacial till activity was the likely cause of the absence of debris flows. On
427 August 23rd, the daily rainfall was 20.3 mm, the antecedent air temperature
428 accumulation dated from DF2, and the active glacial till was still under development.
429 On September 6th, the antecedent positive air temperature accumulation was smaller,
430 and a low air temperature had emerged previously; however, the high rainfall intensity
431 supplemented this lack of prolonged high air temperature.



432 **5. Conclusion**

433 Climate changes have serious effects on high mountainous areas, and mass
434 movement of sediments such as periglacial debris flows is increasingly frequent.
435 Prolonged increases in the annual air temperature are regarded as very favourable for
436 periglacial debris flows. In particular, the annual “hot-dry” weather condition one or
437 two year earlier was responsible for the three debris flow events in Tianmo valley.
438 Debris flow is usually not initiated in the first year because the melting of internal ice
439 particles lags behind the glacial retreat result from the prolong air temperature rise.

440 Glacial till is unlimited in the deglaciated area, while its activity relies on glacial
441 retreat and internal ice particle melting. Changing of glacial tills induced by
442 increasing air temperature is the first step of periglacial debris flows and glacial till
443 need a four phase experience prior to debris flow occurrence (these include:-
444 glacier-covered glacial till, uncovered and frozen glacial till, active glacial till and
445 debris flows), during which the varied air temperature condition with different factor
446 drives the changing. The annual air temperature can remove glaciers, decrease glacial
447 debuttressing and produce bared glacial till; the activity of the frozen glacial till is
448 quite low and would be enhanced by prolonged high air temperature trends; active
449 glacial till would fail and generate debris flows from multiple triggers, such as rainfall
450 or the continuous percolation of ice melt-water. For periglacial debris flows of a large
451 magnitude, the long-term effect of air temperature is required, although rainfall can
452 shorten the antecedent period and generate debris flows earlier.

453 It is difficult to observe the changes of glacial till in source areas of debris flow,
454 and the analysis of the phase conversion of glacial till in this research is based on the
455 conditions that trigger debris flow and other literatures. Indeed, the meteorological
456 conditions, such as the antecedent air temperature and meteorological triggers that
457 drive the phase conversion are partly overlapped and difficult to distinguish. In the
458 first study, we hope to distinguish the effect of each meteorological condition and
459 more detail study should be done in further research.



460 **Acknowledgements:** This research was supported by the National Natural Science Foundation
461 of China (grant No. 41190084, 41402283 and 41371038) and the “135” project of IMHE, CAS. We
462 wish to acknowledge the editors in the Natural Hazards and Earth System Science Editorial Office
463 and the anonymous reviewers for constructive comments, which helped us in improving the
464 contents and presentation of the manuscript.

465 **References**

466 Åkerman, H. J., and Johansson, M.: Thawing permafrost and thicker active layers in sub-Arctic
467 Sweden. *Permafrost Periglac*, 19(3), 279-292, 2008.

468 Arenson, L. U., and Springman, S. M.: Mathematical descriptions for the behaviour of ice-rich
469 frozen soils at temperatures close to 0 °C. *Can Geotech J*, 42(2), 431-442, 2005.

470 Chen, N. S., Zhou, H. B., and Hu, G. S.: Development Rules of Debris Flow under the Influence
471 of Climate Change in Nyingchi. *Adv Clim Change Res*, 7(6), 412-417, 2011. (In Chinese)

472 Chen, R.: Initiation and the critical condition of Glacial debris flow. Master thesis. Institute of
473 Mountain Hazards and Environment, Chinese Academic of Sciences. P19, 1991.

474 Cheng, Z. L., Wu, J. S., and Geng, X.: Debris flow dam formation in southeast Tibet. *J Mt Sci*,
475 2(2), 155-163, 2005.

476 Chiarle, M., Iannotti, S., Mortara, G., and Deline, P.: Recent debris flow occurrences associated
477 with glaciers in the Alps. *Global Planet Change*, 56:123-136, 2007.

478 Christian, B., Philipp, F., and Hansruedi, S.: Thaw-Consolidation Effects on the Stability of Alpine
479 Talus Slopes in Permafrost. *Permafrost Periglac*, 23, 267-276, 2012.

480 Cossart, E., Braucher, R., Fort, M., Bourlès, D. L., and Carcaillet, J.: Slope instability in relation to
481 glacial debuttressing in alpine areas (Upper Durance catchment, southeastern France):
482 Evidence from field data and 10Be cosmic ray exposure ages. *Geomorphology*, 95, 3-26,
483 2008.

484 Cruden, D. M., and Hu, X. Q.: Exhaustion and steady state models for predicting landslide hazards
485 in the Canadian Rocky Mountains. *Geomorphology*, 8, 279-285, 1993.

486 Davies, M., Hamza, O., and Harris, C.: The effect of rise in mean annual temperature on the
487 stability of rock slopes containing ice-filled discontinuities. *Permafrost Periglac*, 12(1),
488 137-144, 2001.

489 Deng, M. F., Chen, N. S., Ding, H. T., and Zhou, C. C.: The Hydrothermal Condition of 2007
490 Group-occurring Debris Flows and Its Triggering Mechanism in Southeast Tibet. *J Nat Dissa*,
491 22(4), 128-134, 2013. (In Chinese)



492 Decaulne, A., and Sæmundsson, T.: Spatial and temporal diversity for debris-flow meteorological
493 control in subarctic oceanic periglacial environments in Iceland. *Earth Surf Proc Land*,
494 32(13), 1971-1983, 2007.

495 Decaulne, A., Sæmundsson, T., Petursson, O.: Debris flows triggered by rapid snowmelt in the
496 Gleidarhjalli area, northwestern Iceland. *Geografiska Annaler*, 87A, 487-500, 2005 .

497 Evans, S. G., Tutubalina, O., Drobyshev, V. N., Chernomorets, S. S., McDougall, S., Petrakov, D.
498 A., and Hungr, O.: Catastrophic detachment and high-velocity long-runout flow of Kolka
499 Glacier, Caucasus Mountains, Russia in 2002. *Geomorphology*, 105(3), 314-321, 2009.

500 Fischer, L., Purves, R. S., Huggel, C., Noetzli, J., and Haeberli, W.: On the influence of
501 topographic, geological and cryospheric factors on rock avalanches and rockfalls in
502 high-mountain areas. *Nat Hazard Earth Sys*, 12(1), 241-254, 2012.

503 Ge, Y. G., Cui, P., Su, F. H., Zhang, J. Q., Chen, X. Z.: Case history of the disastrous debris flows
504 of Tianmo Watershed in Bomi County, Tibet, China: Some mitigation suggestions *J Mt Sci*,
505 11(5), 1253-1265, 2014.

506 Gruber, S., and Haeberli, W.: Permafrost in steep bedrock slopes and its temperature-related
507 destabilization following climate change. *J Geophys Res*, 112, (F02S18), 2007.

508 Guzzetti, F., Peruccacci, S., Rossi, M., and Stark, C. P.: The rainfall intensity-duration control of
509 shallow landslides and debris flows: an update. *Landslides*, 5, 3-17, 2008.

510 Harris, C., Arenson, L. U., Christiansen, H. H., Etzelmüller, B., Frauenfelder, R., Gruber, S., ...
511 and Isaksen, K.: Permafrost and climate in Europe: Monitoring and modeling thermal,
512 geomorphological and geotechnical responses. *Earth Sci Rev*, 92, 117-171, 2009.

513 Harris, C., and Lewkowicz, A. G.: An analysis of the stability of thawing slopes, Ellesmere Island,
514 Nunavut, Canada. *Can Geotech J*, 37(2), 449-462, 2002.

515 IPCC. Summary for policymakers. Working group I contribution to the IPCC Fifth assessment
516 report climate change 2013: the physical science basis. Cambridge, UK: Cambridge
517 University Press, 2013.

518 Iverson, R. M., Reid, M. E., and LaHusen, R. G.: Debris-flow mobilization from landslides. *Annu
519 Rev Earth Pl Sci*, 25(1), 85-138, 1997.

520 Jakob, M.: A size classification for debris flows. *Engineering geology*, 79(3), 151-161, 2005.

521 Jakob, M., Bovis, M., and Oden, M.: The significance of channel recharge rates for estimating
522 debris-flow magnitude and frequency, *Earth Surf. Proc. Land.*, 30, 755-766, 2005.

523 Li, Q. Y., and Xie, Z. C.: (2006) Analysis on the characteristics of the vertical lapse rates of
524 temperature. Taking Tibetan Plateau and its adjacent area as an example. *J Shihezi University
525 (Natural Science)*, 24 (6), 719-723, 2006. (In Chinese).



526 Kean, J. W., McCoy, S. W., Tucker, G. E., Staley, D. M., and Coe, J. A.: Runoff generated debris
527 flows: observations and modeling of surge initiation, magnitude, and frequency. *J Geophys*
528 *Res*, 118, 2190-2207, 2013.

529 Korup, O., and Clague, J. J.: Natural hazards, extreme events, and mountain topography.
530 *Quaternary Sci Rev*, 28, 977-990, 2009.

531 Lewkowicz, A. G., and Harris, C.: Frequency and magnitude of active-layer detachment failures in
532 discontinuous and continuous permafrost, northern Canada. *Permafrost Periglac*, 16(1),
533 115-130, 2005.

534 Liu, J. J., Cheng, Z. L., and Su, P. C.: The relationship between air temperature fluctuation and
535 Glacial Lake Outburst Floods in Tibet, China. *Quatern Int*, 321, 78-87, 2014.

536 Liu, Y.: Research on the typical debris flows chain based on RS in Palongzangbu Basin of Tibet.
537 Chengdu University of Science and Technology, Master thesis, 2013. (In Chinese)

538 Lu, R. R., and Li, D. J.: Ice-Snow-Melt Debris Flows in the Dongru Longba, Bomi county, Xizang.
539 *J Glac Geocry*, 11(2), 148-160, 1989. (In Chinese)

540 McColl, S. T.: Paraglacial rock-slope stability. *Geomorphology*, 153-154, 1-16, 2012.

541 Noetzli, J., Gruber, S., Kohl, T., Salzmann, N., and Haeberli, W.: Three-dimensional distribution
542 and evolution of permafrost temperatures in idealized high-mountain topography. *J Geophys*
543 *Res*, 112, F02S13, 2007.

544 Rahardjo, H., Leong, E. C., and Rezaur, R. B.: Effect of antecedent rainfall on pore-water pressure
545 distribution characteristics in residual soil slopes under tropical rainfall. *Hydrol Process*,
546 22(4), 506-523, 2008.

547 Rango, A., and Martinec, J.: Revisiting the degree-day method for snowmelt computations.
548 *JAWRA Journal of the American Water Resources Association*, 31(4), 657-669, 1995.

549 Rist, A.: Hydrothermal processes within the active layer above alpine permafrost in steep scree
550 slopes and their influence on slope stability. Unpublished PhD thesis, Swiss Federal Institute
551 for Snow and Avalanche Research and University of Zurich, Zurich, 168 pp, 2007.

552 Ryzhkin, I. A., and Petrenko, V. F.: Physical mechanisms responsible for ice adhesion. *J Phys*
553 *Chem B*, 101(32), 6267-6270, 1997.

554 Sassa, K., and Wang, G. H.: Mechanism of landslide-triggered debris flows: Liquefaction
555 phenomena due to the undrained loading of torrent deposits[M]//Debris-flow hazards and
556 related phenomena. Springer Berlin Heidelberg. 81-104, 2005.

557 Sattler, K., Keiler, M., Zischg, A., and Schrott, L., On the connection between debris flow activity
558 and permafrost degradation: a case study from the Schnalstal, South Tyrolean Alps,
559 Italy. *Permafrost Periglac*, 22(3), 254-265, 2011.



560 Schneuwly-Bollschweiler, M., and Stoffel, M.: Hydrometeorological triggers of periglacial debris
561 flows in the Zermatt valley (Switzerland) since 1864. *J Geophys Res*, 117, F02033, 2012.

562 Shang, Y. J., Yang Z. F., Li, L., Liu, D. A., Liao, Q., Wang, Y.: A super-large landslide in Tibet in
563 2000: background, occurrence, disaster, and origin. *Geomorphology*, 54(3), 225-243, 2003.

564 Springman, S. M., Jommi, C., and Teyssiere, P.: Instabilities on moraine slopes induced by loss of
565 suction: a case history. *Géotechnique*, 53(1), 3-10, 2003.

566 Stoffel, M., Bollschweiler, M., and Beniston, M.: Rainfall characteristics for periglacial debris
567 flows in the Swiss Alps: past incidences–potential future evolutions. *Climatic Change*,
568 105(1-2), 263-280, 2011.

569 Stoffel, M., and Huggel, C.: Effects of climate change on mass movements in mountain
570 environments. *Prog Phys Geog*, 36(3), 421-439, 2012.

571 Takahashi, T.: Debris flow: mechanics, prediction and countermeasures. CRC Press, 2014.

572 The Ministry of Land and Resources P. R. C.: China Geological Hazard Bulletin(September
573 edition), 2010.

574 Yao, T. D., Thompson, L., Yang, W., Yu, W., Gao, Y., Guo, X., ... and Pu, J.: Different glacier
575 status with atmospheric circulations in Tibetan Plateau and surroundings. *Nature Climate
576 Change*, 2(9), 663-667, 2012.

577 Yang, W., Guo, X., Yao, T., Zhu, M., and Wang, Y. Recent accelerating mass loss of southeast
578 Tibetan glaciers and the relationship with changes in macroscale atmospheric
579 circulations. *Clim Dynam*, 1-11, 2015.

580 Yang, W., Yao, T., Xu, B., Ma, L., Wang, Z., and Wan, M. Characteristics of recent temperate
581 glacier fluctuations in the Parlung Zangbo River basin, southeast Tibetan Plateau. *Chinese
582 Sci Bull*, 55(20), 2097-2102, 2010.

583 Yuan, G.X., Ding, R. W., Shang, Y. J., Zeng, Q. L.: Genesis of the Quaternary accumulations along
584 the Palong section of the Sichuan-Tibet Highway and Their Distribution Regularities.
585 *Geology and Exploration*, 48(1), 170-176, 2012. (In Chinese)

586



587

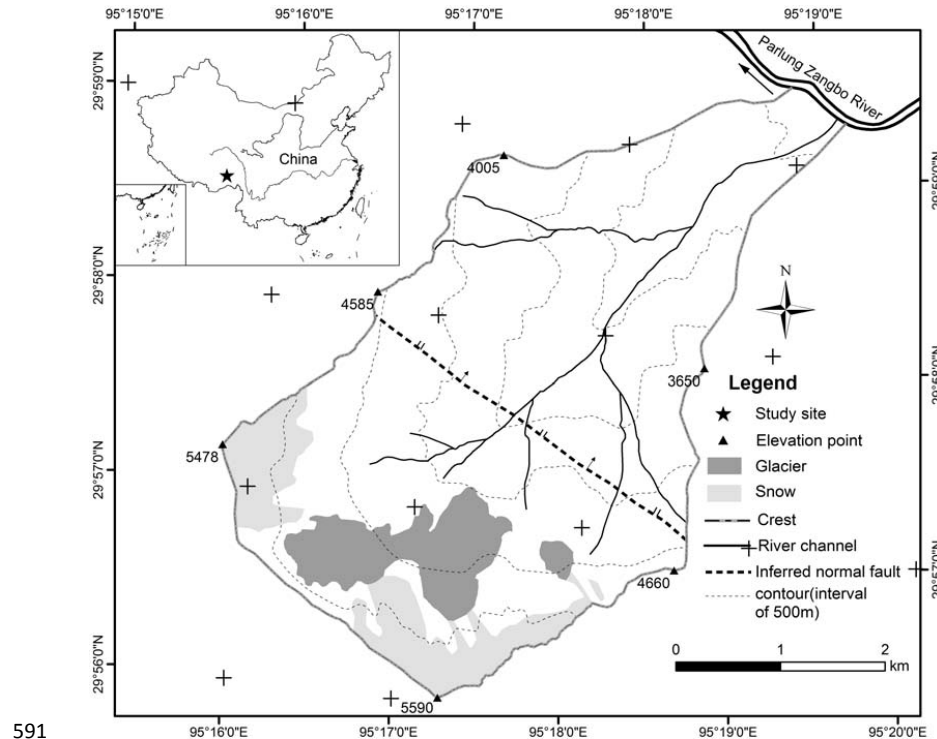
588 Table 1 Changing of glacier, snow, bared land, gully deposition and vegetation in Tianmo valley

Year	Glacier (km ²)	Glacier(eastern branch) (km ²)	Snow (km ²)	Bared land (km ²)	Gully deposition (km ²)	Vegetation (km ²)
2000	1.77	0.16	2.13	2.80	0.44	10.46
2003	1.71	0.15	2.44	2.54	0.44	10.48
2006	1.53	0.12	2.68	2.44	0.44	10.55
2009	1.45	0.096	2.81	3.03	0.47	9.90
2013	1.42	0.088	1.74	3.83	0.51	10.17

589

590 Table 2 Basic information of the debris flows in Tianmo and the nearby valleys

No.	Name	Coordinates	Basin area (km ²)	Glacier area (in 2006) (km ²)	Date	Size class
1	Tianmo valley	29°59'N 95°19'E	17.74	1.53	4 Sep. 2007	6
					25 Jul. 2010	5
					6 Sep. 2010	5
2	Kangbu valley	30°16'N 94°48'E	48.7	1.06	4 Sep. 2007	3
3	Xuewa valley	29°57'N 95°23'E	33.22	0.95	4 Sep. 2007	2
4	Baka valley	29°53'N 95°33'E	22.15	2.46	7 Sep. 2007	3
5	Jiaqing Valley	30°16'N 94°49'E	15.51	1.12	9 Sep. 2007	3



593

594



Figure 2 Overview of the valley from the channel(in 2014)

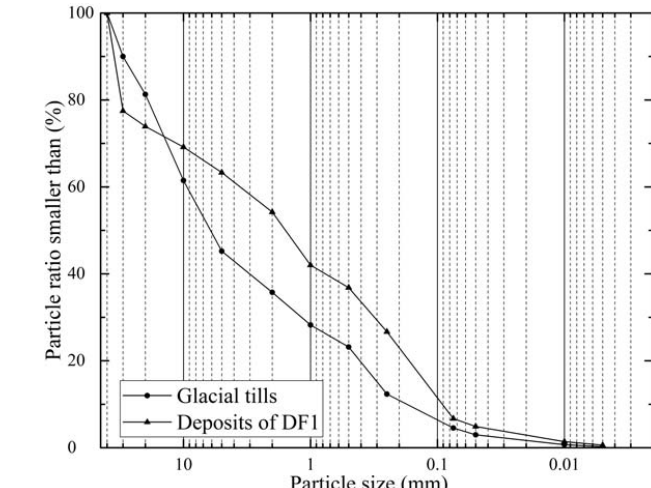


595

596 Figure 3 DF1 in 2007(A. Overview of Tianmo debris flows from the downstream area; B & C.

597 Boulder and debris flow deposits on the north side of the Parlung Zangbo River)

598



599

Figure 4 Particle size distributions of the glacial tills and debris flow deposits

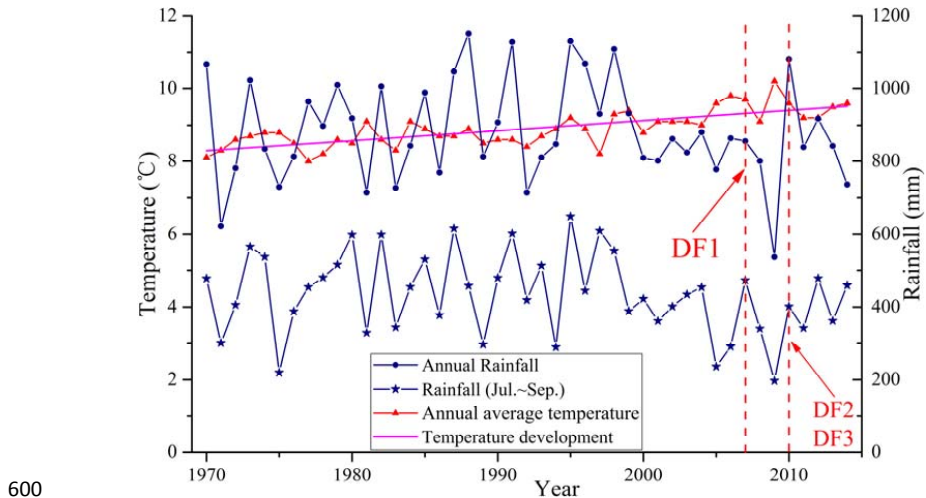


Figure 5 Variation of the annual air temperature and rainfall in Bomi, 1970 to 2014

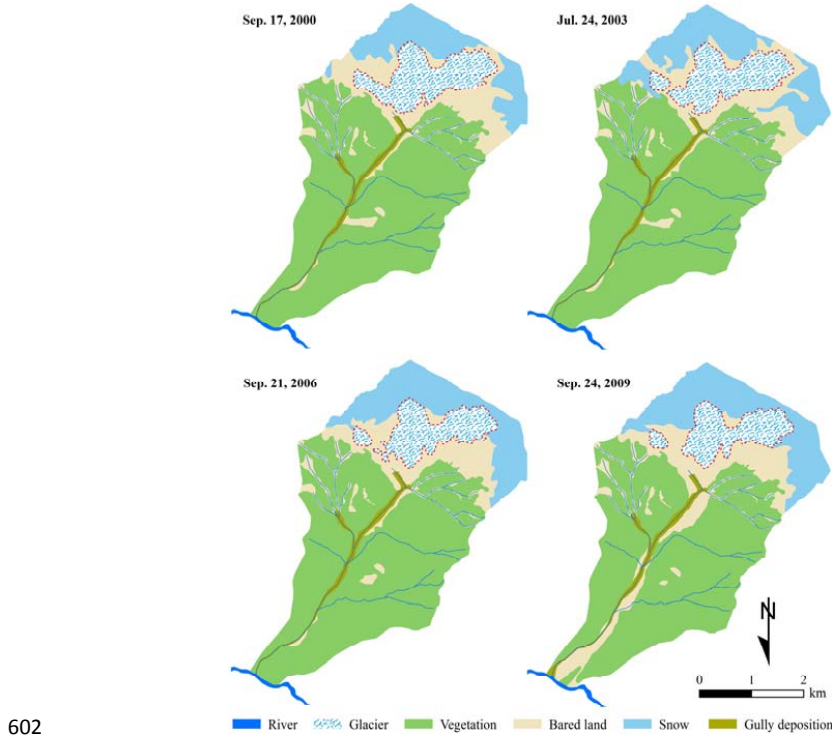
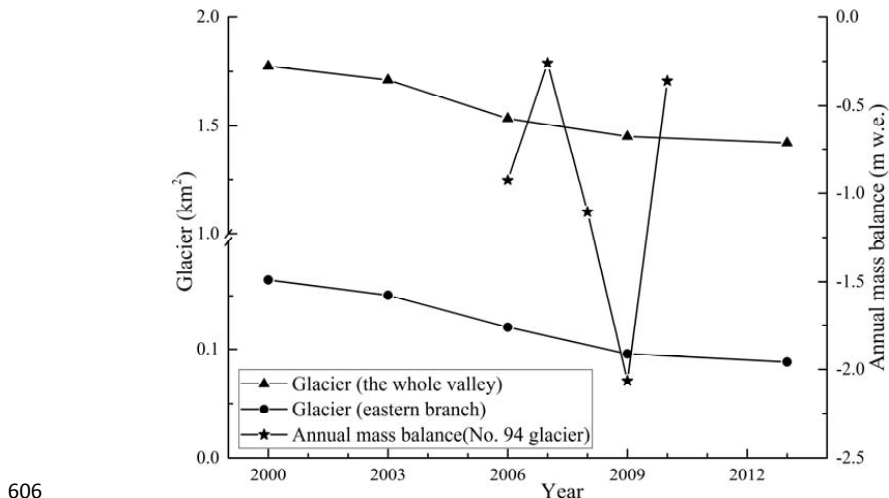
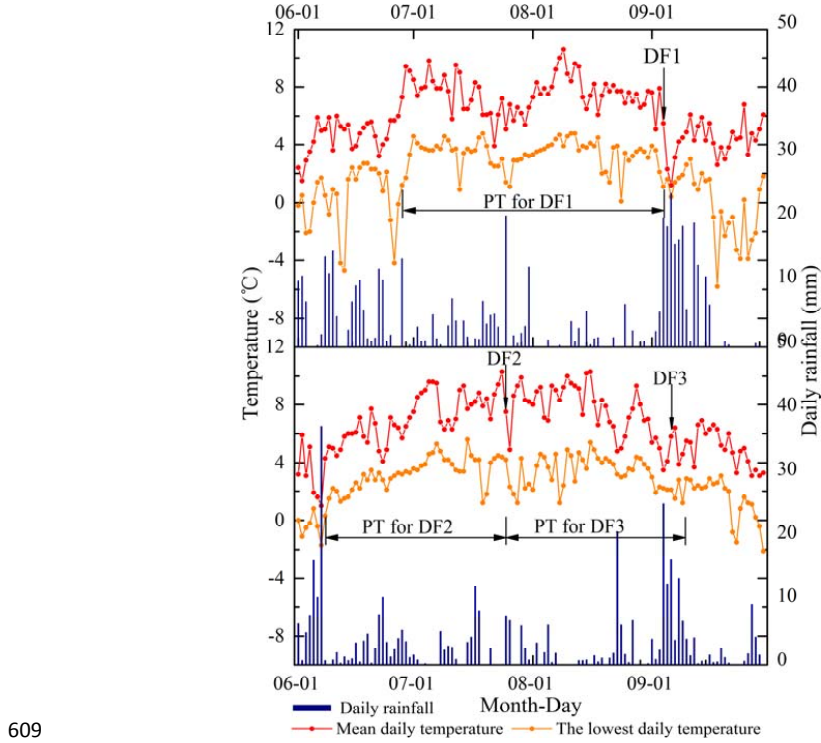


Figure 6 Distribution and changing of glacier, snow, bared land, gully deposition and vegetation in
Tianmo valley



606
607 Figure 7 Changing of glacier via time and the measured annual mass balance for the
608 Parlung No. 94 Glacier (mass balance is edited by Yang et al.(2015))



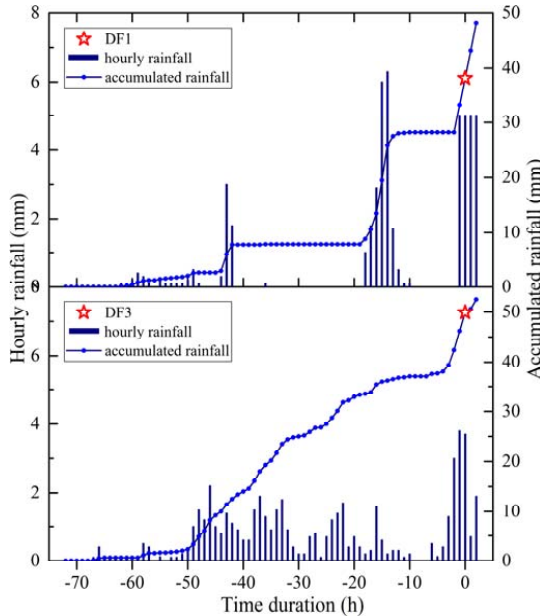
609
610 Figure 8 Air temperature and rainfall before and after DF1, DF2 and DF3



611

612

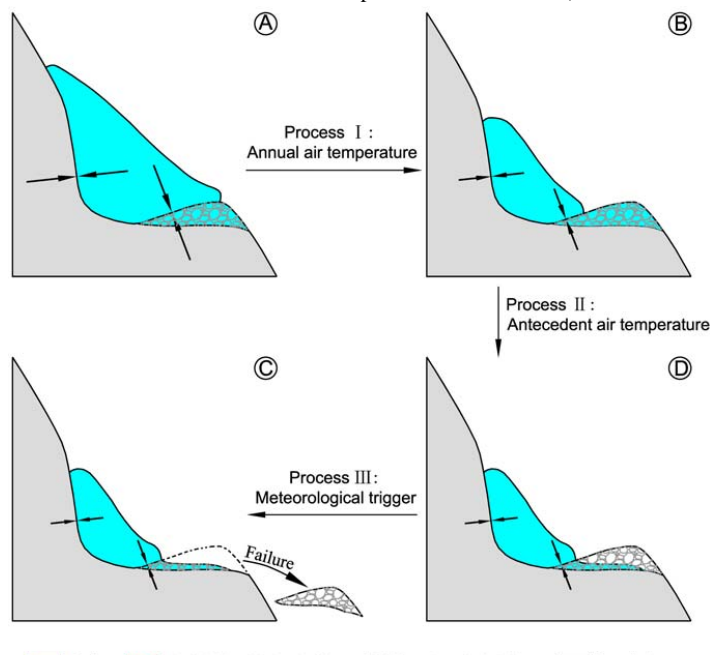
Figure 9 Variation of the rainfall accumulation prior to DF1 and DF3 (no rainfall before DF2)



613

614

615 Figure 10 Changes in a glacier and frozen glacial till before periglacial debris flow initiation (A:
 616 of glacial till)



glacier glacial tills with ice inside active glacial tills basal stress